

# Effect of Hinge Gap Width on the Microflow Structures in 27-mm Bileaflet Mechanical Heart Valves

Hwa-Liang Leo<sup>1</sup>, H el ene A. Simon<sup>2</sup>, Lakshmi P. Dasi<sup>1</sup>, Ajit P. Yoganathan<sup>1,2</sup>

<sup>1</sup>Wallace H. Coulter School of Biomedical Engineering, <sup>2</sup>School of Chemical and Biomolecular Engineering, Cardiovascular Fluid Mechanics Laboratory, Georgia Institute of Technology, Atlanta, Georgia, USA

**Background and aim of the study:** Most bileaflet mechanical heart valves (BMHVs) incorporate some retrograde flow through their hinge mechanism to prevent flow stasis and inhibit microthrombus formation. This reverse flow is characterized by high velocities and shear stresses, thereby promoting platelet activation and hemolysis inside the hinge region. In the present study, the thromboembolic potential of three 27-mm BMHVs with varying hinge gap widths was assessed via in-vitro characterization of the hinge microflow structures.

**Methods:** Three 27-mm BMHV prototypes with different hinge gap widths (50, 100, and 200  $\mu\text{m}$ ) were provided by St. Jude Medical Inc. The valves were mounted in the mitral position of a left heart flow simulator, and two-dimensional laser Doppler velocimetry was used to measure the hinge velocity fields.

**Results:** All three valve prototypes revealed

Despite the success of bileaflet mechanical heart valves (BMHVs), thromboembolic and bleeding complications remain major clinical problems (1,2). Recent studies have shown that the high velocities and elevated turbulent stresses of the leakage flows through these prosthetic heart valves are the primary contributors to the observed clinical problems (3-7). In contrast, leakage flows help wash out the hinge recess, prevent flow stasis, and minimize blood element build-up. This suggests that the hinge region is one of the most critical design features of BMHVs, directly influencing valve functionality and thrombus formation (3-6,8).

Previous studies have focused primarily on the influence of the overall hinge geometry on the flow field (3-7), with few addressing the effect of hinge gap

Reynolds shear stress (RSS) levels above 2,000 dynes/cm<sup>2</sup>, which exceeded the threshold for platelet activation and hemolysis. The hinge flow fields were characterized by leakage jets during systole, and a strong vortical flow during diastole. The leakage jet size and corresponding RSS levels were found to increase with the hinge gap width. All three gap widths had RSS >4,000 dynes/cm<sup>2</sup> (range: 5,640 to 13,315 dynes/cm<sup>2</sup>). The hinge with the smallest gap width registered the highest jet velocity magnitude (2.08 m/s) during systole.

**Conclusion:** The study results showed that the hinge gap width influences washout and RSS levels inside the hinge recess. The 100- $\mu\text{m}$  hinge gap width provided optimum fluid dynamic performance. In contrast, the two valves with large and small hinge gap widths may have higher thromboembolic potential.

The Journal of Heart Valve Disease 2006;15:800-808

width (9-11). When Travis (10) investigated three bileaflet carbon prototypes of the St. Jude Medical (SJM) 27-mm Standard valve, with varying hinge gap width, the smallest and largest hinge gap widths caused higher activated platelet counts than the regular hinge gap width in a steady retrograde blood flow loop. Based on these results, the possible existence was suggested of an optimum hinge gap width. The studies performed by Travis and colleagues did not characterize the hinge flow fields, however, and lacked detailed flow measurements to explain the observed platelet activation levels.

The present study was designed to investigate the influence of hinge gap width on microflow fields within the hinge region, and to relate these results to the potential for blood element damage.

## Materials and methods

### Valve characteristics

Three clear-housing prototypes of the 27-mm

---

Address for correspondence:

Prof. Ajit P. Yoganathan, Department of Biomedical Engineering, Georgia Institute of Technology, 313 Ferst Drive, UA Whitaker Building, Room 2119, Atlanta, Georgia 30332-0535, USA  
e-mail: ajit.yoganathan@bme.gatech.edu

Standard SJM valve with varying hinge gap widths were provided by St. Jude Medical, Inc. (Minnesota, USA). The leaflets of the prototypes were constructed from Delrin and enclosed in a clear housing to ensure optical access to the hinge region. The term 'hinge gap width' was defined as the clearance between the tip of the leaflet ear and the center of the hinge recess (Fig. 1a). The hinge gap widths of the three valves, measured using microcomputed tomography, were approximately 50, 100, and 200  $\mu\text{m}$ , and the valves were designated as the 'low leaker prototype' (LLP), the 'Standard SJM' (Standard), and the 'high leaker prototype' (HLP), respectively.

### Flow velocity measurements

The three valves were mounted in the mitral position of the Georgia Tech left heart simulator, and laser Doppler velocimetry (LDV) measurements were performed at selected elevation planes through the hinge region to measure the velocity fields and quantify turbulence characteristics. The grid spacing between measurement locations inside the hinge recess (above the flat level) was 0.254 mm and 0.381 mm in the x and y directions, respectively, while outside the hinge recess (below the flat level) the grid resolution was 0.394 mm and 0.787 mm in the x and y directions, respectively.

The flow set up used in the present study was typical for an adult human. The specific physiological conditions imposed on the valve included: heart rate of 70 beats/min (corresponding to a cardiac cycle of 860 ms), cardiac output of 4.0 l/min, peak diastolic flow

rate of 10.0 l/min, diastolic duration of 560 ms, and peak left ventricular pressure of 130 mmHg. The compliance and resistance sections of the loop allowed additional control of the mitral flow and pressure waveforms.

The working fluid was a solution of 79% saturated aqueous sodium iodide, 20% glycerin, and 1% water (v/v/v). This blood analogue fluid had a kinematic viscosity of  $3.5 \times 10^{-6} \text{ m}^2/\text{s}$  (3.5 cSt) to match that of blood at high shear rates, and its refractive index was adjusted to match that of the valve-mounting chamber (1.49), thereby minimizing optical distortion. The flow was seeded with silicon carbide particles (TSI Inc., Shoreview, MN, USA) with a nominal diameter of 1.5  $\mu\text{m}$ .

Two-component velocity measurements were obtained with a fiber optic, three-component, coincident LDV system (Aerometrics Inc., CA, USA) used in backscatter mode. A two-component fiber optic transceiver (Model XRV 1204; TSI Inc.) with a 100-mm focal length lens was coupled to a fiber drive to produce an ellipsoidal probe volume with minor and major axes of 21  $\mu\text{m}$  and 140  $\mu\text{m}$ , respectively. A total of 21,500 measurement samples was acquired at each measurement location. Measured velocities were computed off-line using gate time-weighted averaging to eliminate velocity bias. The velocities were phase-averaged within 20-ms time windows for subsequent analysis, each of which contained an average of 500 data points. This temporal resolution was sufficiently long to ensure a valid statistical result in each time window, and yet short enough to consider the data set within each time window as quasi-steady. Statistical filtering was then applied such that samples more than five standard deviations from the mean were discarded. A detailed description of the data processing can be found elsewhere (7,10,12). The selection of the 20-ms bin width used for calculation of statistics is currently the smallest value to achieve both satisfactory temporal resolution and statistical convergence for the hinge study. Since 20-ms temporal resolution does not resolve the opening and closing events, the study was focused on the influence of hinge gap width only on the flow phases consistently studied previously (3,5,6) to determine the thromboembolic potential of hinge designs under mitral conditions.

In addition to the pulsatile experiments described above, the three valves were tested under static pressure conditions. Each valve was subjected to a constant back-pressure of 120 mmHg using a constant-head reservoir, and the leakage flow rate measured using a bucket and stop watch. The working fluid was a water/glycerin blood analogue solution (60/40, v/v). The leakage flow rate was computed as an average of six repetitions of the experiment.

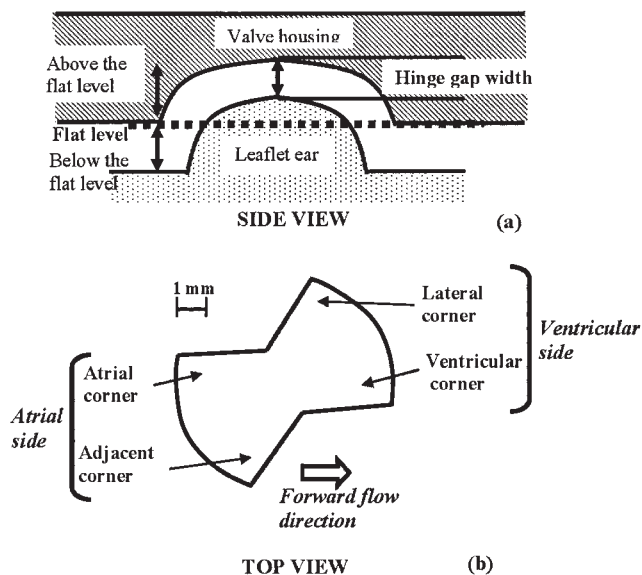


Figure 1: Side view (a) and top view (b) schematics of the hinge region, with pertinent terminology used to describe the laser Doppler velocimetry (LDV) measurement locations.

## Results

### Static leakage rate experiments

The highest and lowest leakage flow rates observed were from the 27-mm HLP and LLP valves, with average values of  $0.490 \pm 0.021$  l/min and  $0.049 \pm 0.001$  l/min, respectively. The leakage rate for SJM 27-mm Standard ( $0.351 \pm 0.022$  l/min) was between that of the HLP and LLP valves.

### Flow velocity measurements inside and outside the hinge pivot

The results are presented as two-dimensional vector plots, illustrating the phase-averaged in-plane velocity field at specific phases of the cardiac cycle, namely the systolic (leaflets in closed position) and diastolic (leaflets in open position) phases. For clarity, the leaflets were not superimposed on the plots. The arrows pointed in the direction of the mean velocity vectors and are color-coded by the Reynolds shear stress (RSS) magnitude given in the figure legends. The arrow lengths were proportional to the velocity magnitude. The terminology used to describe the geometry of the hinge is indicated in Figure 1b. The overall fluid dynamic effect of hinge gap width is depicted by the velocity and RSS fields at the flat level, and at 190 and 390  $\mu\text{m}$  above the flat level. Results at different elevations below the flat level showed similar flow patterns, and therefore description of the results below the flat levels is limited to that of the flow field recorded at 500  $\mu\text{m}$  below the flat level. Results for the 27-mm Standard valve are followed by those of the LLP and HLP.

#### 27-mm Standard SJM valve at the flat level

**Systole:** A leakage jet of 0.60 m/s was seen in the atrial corner of the hinge geometry at the onset of systole. Approaching mid-systole (Fig. 2a), this leakage jet

reached a peak velocity of 1.40 m/s, while the maximum velocity recorded in the leakage jet at the adjacent corner was smaller (1.10 m/s). Regions of low flow ( $<0.05$  m/s) were observed along the hinge boundary at the atrial and ventricular corners. The calculated RSS levels in the atrial jet ranged from 100 to 1,100 dynes/cm<sup>2</sup> (Fig. 2a), while the RSS levels in the adjacent jet were between 1,000 and 5,500 dynes/cm<sup>2</sup>. A third jet, observed in the lateral corner had a peak velocity magnitude of 0.37 m/s and a corresponding RSS level of 300 dynes/cm<sup>2</sup>.

**Diastole:** A vortical flow, with a velocity magnitude on the order of 0.50 m/s and RSS values ranging between 10 and 250 dynes/cm<sup>2</sup>, was observed at the adjacent corner at mid-diastole (Fig. 2b). The velocity magnitudes and RSS levels of the low flow observed in the lateral and ventricular hinge corners were 0.05 m/s and 10 dynes/cm<sup>2</sup>, respectively.

#### 27-mm Standard SJM valve at 190 $\mu\text{m}$ above the flat level

**Systole:** The flow trend observed at 190  $\mu\text{m}$  above flat level was similar to that at the flat level. Figure 3a shows the flow field at early systole. Approaching mid-systole, the leakage jet at the atrial corner reached a maximum velocity of 1.34 m/s, but abruptly reduced in size and velocity magnitude towards the end of systole. The leakage jet at the adjacent corner reached a velocity of 0.9 m/s at mid-systole. The RSS levels throughout the hinge region were typically  $<100$  dynes/cm<sup>2</sup>, except at the atrial and adjacent leakage jets where peak RSS levels up to 1,000 and 3,800 dynes/cm<sup>2</sup>, respectively were recorded.

**Diastole:** A vortical flow, with a peak velocity magnitude of 0.16 m/s and a corresponding RSS value  $<10$  dynes/cm<sup>2</sup>, was visible at the adjacent corner of the

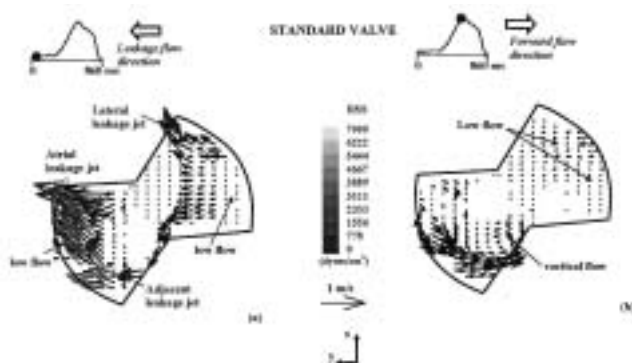


Figure 2: Phase-averaged mitral velocity field (shown as vectors) and Reynolds shear stress (RSS) distribution (color-coded) at the flat level of the hinge region for the Standard valve at (a) approaching mid-systole and (b) mid-diastole. Cardiac phases represented as a ball on the flow curve.

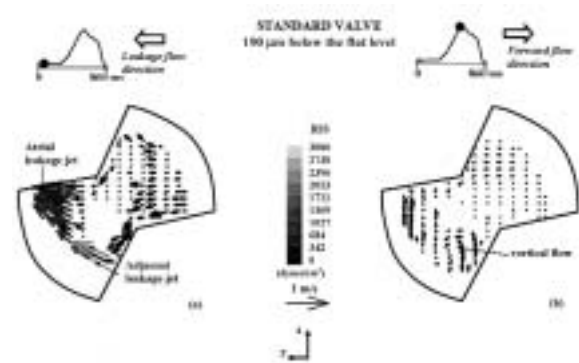


Figure 3: Phase-averaged mitral velocity field (shown as vectors) and Reynolds shear stress (RSS) distribution (color-coded) at 190  $\mu\text{m}$  above the flat level of the hinge region for the Standard valve at (a) approaching mid-systole and (b) mid-diastole. Cardiac phases represented as a ball on the flow curve.

hinge geometry (Fig. 3b). Flow at other measurement locations inside the hinge had a low velocity of 0.02 m/s and corresponding RSS levels <10 dynes/cm<sup>2</sup>.

**27-mm Standard SJM valve at 390 μm above the flat level**

**Systole:** The flow field at 390 μm above the flat level was characterized by flow velocities ranging from 0.02 to 0.7 m/s. A maximum leakage velocity of 0.76 m/s and a corresponding RSS value of 1,261 dyne/cm<sup>2</sup> were recorded at the ventricular side during early systole. Leakage flow (>0.14 m/s) was observed along the ventricular edge of the hinge at mid-systole, and persisted to end of systole. Here, the RSS levels were generally <5 dynes/cm<sup>2</sup>.

**Diastole:** The flow velocity during diastole was typically <0.12 m/s, but a band of slightly higher velocity flow (0.14 m/s) was observed along the atrial edge of the hinge wall. The RSS values were <10 dynes/cm<sup>2</sup>.

**27-mm Standard SJM valve at 500 μm below the flat level**

**Systole:** Two leakage jets emanating from the hinge recesses and a third slower jet emanating from the gap between the two leaflets, called the B-datum line, were apparent during systole (Fig. 4a). The leakage jets arising from the hinge recesses had a maximum velocity of 2.10 m/s, and corresponding RSS levels ranging from 1,000 to 2,000 dynes/cm<sup>2</sup>. The central orifice leakage jet, emanating from the B-datum line, reached a maximum velocity of 0.20 m/s and a corresponding maximum RSS level of 2,590 dynes/cm<sup>2</sup>.

**Diastole:** The flow at the start of diastole was characterized by a strong central orifice jet and two side jets, which reached velocities of 0.90 m/s and 1.25 m/s, respectively, during mid-diastole (Fig. 4b). At this

phase of the cardiac cycle, a maximum RSS level of 1,000 dynes/cm<sup>2</sup> was seen in the central forward flow jet, while the RSS levels in the regions bounded by the central and side forward jets were 100 dynes/cm<sup>2</sup>.

**27-mm Low Leaker Prototype (LLP) at the flat level**

**Systole:** The flow field distribution observed during systole was qualitatively similar to that in the Standard valve. At mid-systole, the leakage jet at the atrial corner reached a velocity magnitude of approximately 0.60 m/s, and corresponding RSS levels ranged from 500 to 900 dynes/cm<sup>2</sup> (Fig. 5a). A smaller but faster jet with a maximum velocity of 2.08 m/s was measured at the adjacent corner at mid-systole, with RSS levels ranging between 1,000 and 3,000 dynes/cm<sup>2</sup>. The RSS levels in the ventricular and lateral corners were typically <20 dynes/cm<sup>2</sup>.

**Diastole:** The flow field distribution during diastole was again qualitatively similar to that observed in the Standard valve. The velocity during the acceleration phase was generally <0.05 m/s throughout the hinge geometry. A region of vortical flow became apparent around mid-diastole at the adjacent corner, with the eye of the vortex lying next to the leaflet ear. The flow velocity of the vortical flow reached a maximum velocity of 0.43 m/s at mid-diastole. The RSS levels throughout the measurement plane ranged from 10 to 100 dynes/cm<sup>2</sup> during diastole.

**27-mm Low Leaker Prototype (LLP) at 190 μm above the flat level**

**Systole:** The flow patterns of the LLP at 190 μm above the flat level were similar to those observed in the same valve at the flat level. Leakage jets were observed at the atrial and adjacent corners of the hinge geometry. A maximum velocity magnitude of 0.91 m/s was

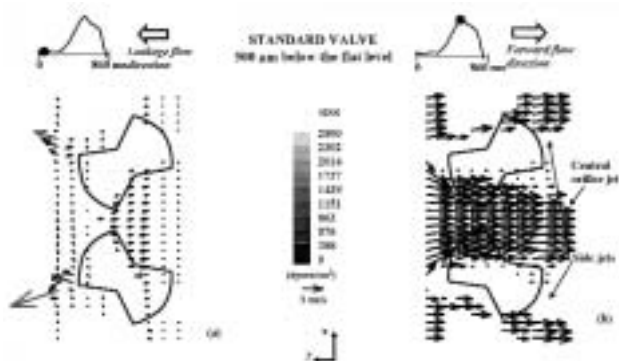


Figure 4: Phase-averaged mitral velocity field (shown as vectors) and Reynolds shear stress (RSS) distribution (color-coded) at 500 μm below the flat level of the hinge region for the Standard valve at (a) approaching mid-systole and (b) mid-diastole. Cardiac phases represented as a ball on the flow curve.

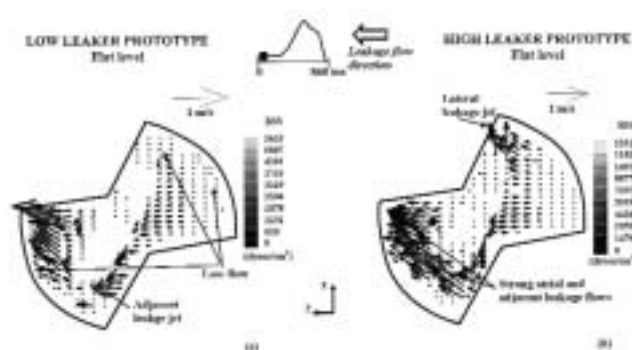


Figure 5: Phase-averaged mitral velocity field (shown as vectors) and Reynolds shear stress (RSS) distribution (color-coded) at the flat level of the hinge region for the low leaker prototype (LLP) (a), and high leaker prototype (HLP) (b), approaching mid-systole. Cardiac phase represented as a ball on the flow curve.

recorded at the atrial corner toward mid-systole, while a smaller leakage jet of 1.03 m/s was seen developed at the adjacent corner (Fig. 6a). The ventricular and lateral corners were characterized by near-zero velocity flow that persisted throughout systole. A maximum RSS of 4,146 dynes/cm<sup>2</sup> was recorded in the adjacent leakage jet. The RSS values at the adjacent corner were much higher (1,500-4,150 dynes/cm<sup>2</sup>) than that at the atrial corner (400-500 dynes/cm<sup>2</sup>).

*Diastole:* A vortical flow persisted at the adjacent corner throughout diastole, but became weaker towards the end of diastole. A strong forward flow (0.4 m/s) was observed at the atrial side and was directed around the leaflet ear towards the vortical flow. The ventricular and lateral corners were characterized by near-zero velocity flow (0.04 m/s) throughout diastole. The RSS levels during diastole were <24 dynes/cm<sup>2</sup>. The peak RSS value of 24 dynes/cm<sup>2</sup> was recorded at the adjacent corner between the vortical flow and the wall of the hinge geometry.

**27-mm Low Leaker Prototype (LLP) at 390 μm above the flat level**

Low velocity flow was recorded throughout the hinge region during systole, with a maximum velocity of 0.46 m/s observed at the ventricular side. The RSS levels were <10 dynes/cm<sup>2</sup>.

Velocity magnitudes during diastole were on the order of 0.04 m/s, and the RSS levels were <10 dynes/cm<sup>2</sup>.

**27-mm Low Leaker Prototype (LLP) at 500 μm below the flat level**

*Systole:* Three leakage flows were observed throughout systole. At mid-systole, the central leakage flow,

emanating from the B-datum line, had a velocity of 0.20 m/s and a corresponding peak RSS level of 500 dynes/cm<sup>2</sup>. The two lateral leakage flows emanating from the hinge recesses reached a peak velocity of 0.70 m/s and corresponding maximum RSS level of 1,440 dynes/cm<sup>2</sup>.

*Diastole:* During diastole, the flow field distribution was characterized by a central jet and two side jets. All three jets reached a velocity magnitude of 1.0 m/s at peak diastole. The RSS levels in the central and side jets were <100 dynes/cm<sup>2</sup> at the onset of diastole, and decreased to 10 dynes/cm<sup>2</sup> during the rest of diastole.

**27-mm High Leaker Prototype (HLP) at the flat level**

*Systole:* The flow field at the flat level of the HLP during early systole was qualitatively similar to that observed in the Standard valve and the LLP, except that higher velocity magnitudes and larger leakage jets were measured at both the atrial and adjacent corners (Fig. 5b). At mid-systole the atrial jet reached a maximum velocity of 1.86 m/s, while the peak velocities in the adjacent and lateral corners were 1.57 and 0.96 m/s, respectively. The RSS levels reached 4,000 dynes/cm<sup>2</sup> in the adjacent jet, while in the atrial and side jets, the peak RSS levels recorded were three- to six-fold smaller at 1,440 and 700 dynes/cm<sup>2</sup>, respectively.

*Diastole:* The velocities at the flat level of the HLP during diastole were lower than those recorded in the Standard and LLP valves. Velocities throughout the hinge region were close to zero during diastole, except in the vortical flow at the adjacent corner where a maximum flow velocity of 0.20 m/s was recorded. The RSS levels throughout the hinge were typically <10 dynes/cm<sup>2</sup>.

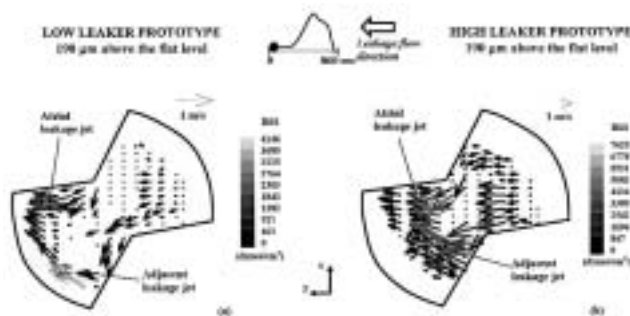


Figure 6: Phase-averaged mitral velocity field (shown as vectors) and Reynolds shear stress (RSS) distribution (color-coded) at 190 μm above the flat level of the hinge region for the low leaker prototype (LLP) (a), and high leaker prototype (HLP) (b), approaching mid-systole. Cardiac phase represented as a ball on the flow curve.

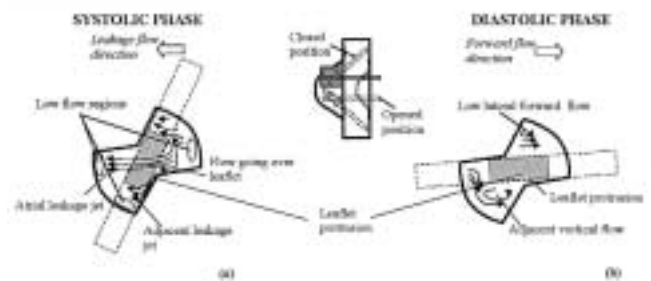


Figure 7: Schematic of the common flow features inside the hinge recess of the three valves. (a) during systole; (b) during diastole.

### 27-mm High Leaker Prototype (HLP) at 190 $\mu\text{m}$ above the flat level

*Systole:* The observed flow pattern was similar to that seen at the flat level, and also at both the flat and 190  $\mu\text{m}$  above the flat levels of the Standard and LLP valves (Fig. 6b). Two main leakage jets were seen in the hinge at the atrial corner and the adjacent corner. The leakage flow in the ventricular side reached a maximum velocity of 1.95 m/s towards mid-systole, while those at the atrial and adjacent corners fluctuated between 0.3 and 1.2 m/s. The observed flow field persisted until late systole. The RSS levels of the leakage jets at the atrial and adjacent corners varied between 1,000 and 7,500 dynes/cm<sup>2</sup>, while those in the ventricular and lateral corners were lower and ranged from 500 to 2,500 dynes/cm<sup>2</sup>.

*Diastole:* The flow velocity during diastole was typically <0.02 m/s throughout the entire hinge region, and the corresponding RSS levels were <15 dynes/cm<sup>2</sup>. A vortical flow region was observed at the adjacent corner at mid-diastole, and persisted throughout diastole.

### 27-mm High Leaker Prototype (HLP) at 390 $\mu\text{m}$ above the flat level

Near-zero velocities (0.01 m/s) and low RSS levels (<5 dynes/cm<sup>2</sup>) were recorded during systole in the entire hinge region except for the ventricular side, where a strong leakage flow was observed. The leakage jet reached a maximum velocity of 0.85 m/s and a corresponding peak RSS level of 1,147 dynes/cm<sup>2</sup> at mid-systole.

Flow velocities during diastole were <0.02 m/s, with RSS levels close to zero.

### 27-mm High Leaker Prototype (HLP) at 500 $\mu\text{m}$ below the flat level

*Systole:* The systolic flow field was similar to those

observed in the other two valves at the same elevation. The two leakage jets emanating from the hinge recesses reached a peak velocity of 1.00 m/s at mid-systole, with a corresponding RSS level of 1,320 dynes/cm<sup>2</sup>. The central leakage flow was slower, with a peak velocity of 0.25 m/s and a corresponding RSS level of 100 dynes/cm<sup>2</sup>.

*Diastole:* The flow field distribution throughout diastole was similar to those observed with the Standard and the LLP valves. The maximum velocity in the three forward jets reached 1.00 m/s, and the corresponding RSS levels ranged from 30 to 100 dynes/cm<sup>2</sup> during mid-diastole.

## Discussion

### Effect on static leakage flow

The static leakage performance of the three 27-mm bileaflet valves showed that the leakage flow rate increased with hinge gap width. A closer comparison of the leakage flow rate results revealed that both the Standard and HLP valves had leakage rates that were one order of magnitude higher than that of the LLP valve. Similar experiments on static leakage performance with respect to hinge gap width were conducted by Travis (10) for three 27-mm carbon BMHVs. The leakage rates of the 27-mm carbon HLP and LLP valves were found to be  $0.84 \pm 0.08$  l/min and  $0.147 \pm 0.011$  l/min, respectively (10), with that of the carbon HLP being almost double that of the current HLP clear-housing model. This variation was attributed to differences in the hinge gap widths between the clear-housing and carbon HLPs. The leakage result for the SJM 27-mm Standard carbon valve obtained by Travis was  $0.423 \pm 0.034$  l/min (10). In assessing these results, the clear-housing LLP presents an extreme case for a very low hinge gap width, while the clear-housing HLP valve represents a moderately higher gap width.

Table I: Comparison of numbers of measurement locations at the atrial and adjacent leakage jets at the flat level, with corresponding velocity (m/s) and Reynolds shear stress ranges (dynes/cm<sup>2</sup>, in parentheses) for the three valve types.

Valve type	Systole				Diastole		
	Flat level	Above the flat level ( $\mu\text{m}$ )			Below the flat level ( $\mu\text{m}$ )		
		190	390	585	500	1000	3000
LLP	2.08 (5,630)	1.03 (4,145)	0.39 (490)	NA -	1.24 (1,440)	1.29 (1,370)	1.35 (630)
Standard	1.57 (7,000)	1.34 (3,810)	0.72 (1,260)	0.04 (10.0)	2.1 (2,590)	1.39 (2,070)	1.44 (440)
HLP	1.85 (13,315)	1.94 (7,625)	0.84 (1,150)	0.06 (115)	1.31 (1,320)	1.42 (800)	1.41 (445)

NA: Not available.

**Common flow features**

The maximum phase-averaged velocity magnitudes and RSS levels measured both inside and outside the hinge region are summarized in Table I. For all three valves, the peak velocities within the hinge recess were observed in the atrial and adjacent corners of the hinge during systole, while the maximum velocities outside the hinge recess were generally recorded in the forward flow jets during diastole. The relative sizes of the atrial and adjacent corner leakage jets for the three valves are summarized in Table II; the respective velocity and RSS level ranges observed are also listed. The main flow features observed at and above the flat level within the hinge recess during systole and diastole are summarized in Figure 7.

**Flow field inside the hinge recess**

During early systole at the flat level, leakage jets were observed in the atrial and adjacent corners of all three valve hinge geometries. Even though the adjacent jet was smaller in spatial size than the atrial jet, the RSS levels in the adjacent corner were typically a factor of two higher than those recorded in the atrial corner (Table II). This may be due to the relatively smaller size of the squeeze flow occurring under the leaflet at the adjacent corner of the hinge. The lateral jet flow is also a result of squeeze flow between the leaflet and the edge of the hinge. Low-flow regions with a velocity magnitude of less than 0.05 m/s (see Fig. 7a) were observed along the hinge wall at both the atrial and ventricular corners due to these measurement points lying close to the recess boundary. During diastole, a vortical flow region was observed in the adjacent corner of the hinge at the flat level (Fig. 7b). Fluid from the atrial and adjacent corners appears to enter this vortex and move downstream in a helical manner while crossing the hinge gap. This vortical structure, which has been observed previously (3-6,8,9,13), was also evident in the present study, both at the flat level and at 190 μm above the flat level. The leakage flow patterns at 190 μm above the flat level were similar to those seen at the flat level. During diastole, a vortical flow was observed near the adjacent corner of the hinge at the flat level, and at 190 μm above, the flat level in all

three valves. Flows from the atrial and adjacent corners were directed into this vortical zone as a result of the obstruction of the leaflet ear in the open position.

The peak RSS values (see Table I) were above the critical thresholds estimated for red blood cell damage and platelet activation (3,6,14-17). RSS values reported to cause hemolysis range from 400 to 5,600 dynes/cm<sup>2</sup> with exposure time ranging from 10<sup>-4</sup> to 10<sup>2</sup> s (14,17). The reported values of RSS leading to platelet activation range from 100 to 1,000 dynes/cm<sup>2</sup>, with exposure time ranging from 10<sup>-2</sup> to 10<sup>2</sup> s (15,16). The observed ranges of RSS in the leakage jets at the atrial and adjacent corners during systole were 500-1,500 dynes/cm<sup>2</sup> and >5,000 dynes/cm<sup>2</sup>, respectively (Table II). Therefore, these leakage jets are regions that possibly favor platelet activation and hemolysis. Given that in the present study the velocity was phase-averaged over a time bin of 20 ms (10<sup>-2</sup> s), it is reasonable to assume that the large magnitudes of RSS last for sufficient duration to be detrimental to blood elements.

**Flow field outside the hinge recess**

The flow below the flat level of all three valves was found to be strongly influenced by the leaflet position. During mid-systole, high velocity leakage jets, with peak velocity magnitudes exceeding 1.0 m/s (Table I), were seen emanating from the two hinge recesses and from the B-datum line. The diastolic flow fields at all elevations below the flat level were characterized by three forward flow jets of similar velocity magnitude - one central orifice jet bounded by two side jets. This flow pattern, which is typical of a BMHV, was a result of the open leaflet configuration during the forward flow phase.

The flow velocities and RSS levels measured below the flat level were typically lower than those within the hinge recess (Table I). At these elevations, the regions most likely to cause blood element damage were the systolic leakage jets - two emanating from the hinge recess and one from the B-datum line.

**Differences in flow features and RSS levels**

There was no noticeable difference in the flow fields below the flat level for the three valves. The largest dif-

Table II: Peak phase-averaged velocity (m/s) and Reynolds shear stress (RSS; dynes/cm<sup>2</sup>) for the three valve types.

Valve type	Leakage jets	Measurement locations (n)	Velocity range (m/s)	RSS range (dynes/cm <sup>2</sup> )
LLP	Atrial jet	32	0.26-0.71	110-1,000
	Adjacent jet	8	0.28-2.08	200-3,050
Standard	Atrial jet	34	0.35-1.57	160-2,360
	Adjacent jet	10	0.27-1.1	130-3,475
HLP	Atrial jet	39	0.35-1.85	400-2,825
	Adjacent jet	19	0.34-1.57	1,017-4,830

ferences were observed within the hinge recess. During mid-systole, the atrial leakage jet at the flat level of the HLP was larger and had higher velocities than those observed in the Standard and LLP valves (Table II). In addition, during early systole the leakage jets at the atrial and adjacent corners in both the Standard and HLP valves experienced an averaged RSS of about 40% and 228%, respectively, higher than that observed for the LLP. These two observations may be attributed to the larger hinge gap widths of the HLP and Standard valves compared to the LLP, thereby allowing a larger jet to originate from the center of the hinge recess.

During diastole, BMHVs with large hinge gap widths (e.g., those of the HLP), when implanted in the mitral position, might have an increased risk of thrombus build-up in the hinge region due to the reported lower forward flow velocities. The lower forward flow through the mitral valve may make the prosthesis vulnerable to thrombus build-up in the hinge region, and this supports the clinical observation that mitral valves have higher incidences of thromboembolic and bleeding complications than aortic valves (18,19).

In contrast, compared to the HLP and Standard valves, the LLP had the smallest leakage jet size, though the recorded peak velocity (2.08 m/s) was the highest among all valves (Table I). This may predispose the LLP to an increased risk of blood element damage.

#### **Integration of previous blood experiments with the observed flow structures**

Previously, Travis and colleagues assessed the effect of the hinge gap width on blood damage and platelet activation under steady leakage flow conditions (10,11). These authors found that both the HLP and LLP had higher activated platelet counts than the Standard SJM valve, and concluded that the hinge gap width influenced both platelet activation and anionic phospholipid exposure due to leakage flow alone. Although the activated platelet count difference between the Standard valve and LLP was not significant, the HLP was shown to activate significantly more platelets than the Standard valve. Travis et al. also postulated that different mechanisms might be responsible for the observed elevated platelet activation seen in both the HLP and LLP (11). In the HLP, this elevation may be due to greater turbulence inside the hinge recess as a result of the increased hinge gap width, whereas in the LLP the dominant force behind the observed platelet activation might be the viscous shear stresses. In fact, the results of the present study corroborated the hypotheses of Travis and colleagues, and showed that the HLP had comparatively larger regions of elevated RSS levels than did either the Standard or LLP valve.

The maximum calculated viscous shear stresses based on the maximum velocity measured in the hinge of the HLP, Standard and LLP valves were 1,350, 2,300 and 5,880 dynes/cm<sup>2</sup>, respectively. Details of these calculations may be found in the literature (20). The LLP valve had a higher viscous shear stress level than the other two valves, and this may be responsible for the increased platelet activation reported by Travis et al. (11).

*In conclusion*, the present study examined the effect of hinge gap width on the microflow fields of BMHVs, and shows the performance of the 27-mm Standard SJM valve to lie between that of the HLP and LLP valves. From a fluid dynamics perspective, the Standard valve has a more optimal hinge gap width than the other valves. The results also suggest a potential for inefficient washout of blood elements in valves with large hinge gap widths, as shown by the lower velocity magnitudes observed. Compared to the Standard and LLP valves, the hinge of the HLP was plagued by higher velocity magnitudes and elevated RSS during systole. In contrast, the LLP recorded smaller regions of high RSS and elevated velocities than the other valves, though its smaller hinge gap width may make it more prone to blood element damage owing to increased viscous shear stresses. Regions of high RSS were typically formed during systole both inside and outside the hinge region. These regions were at the atrial and adjacent leakage jets inside the hinge recess, and in the flow from the B-datum line below the flat level. The RSS levels in these regions were above the threshold for hemolysis and platelet activation, and therefore may induce blood cell activation. Overall, the present study highlighted the importance of hinge gap width in determining the hemodynamic performance of a BMHV, and revealed that a hinge design with optimal tolerances may significantly reduce the potential for thrombus formation.

#### **Acknowledgements**

These studies were funded by a gift from Tom and Shirley Gurley and by NHLBI grant # HL70262-02.

#### **References**

1. Vongpatanasin W, Hillis LD, Lange RA. Prosthetic heart valves. *N Engl J Med* 1996;335:407-416
2. Yoganathan AP. Cardiac valve prostheses. In: *The Biomedical Engineering Handbook*. 2nd edn. CRC Press LLC, 2000:127-1-127-23
3. Ellis JT, Healy TM, Fontaine AA, Saxena R, Yoganathan AP. Velocity measurements and flow patterns within the hinge region of a Medtronic Parallel bileaflet mechanical valve with clear housing. *J Heart Valve Dis* 1996;5:591-599

4. Ellis JT, Healy TM, Fontaine AA, et al. An in vitro investigation of the retrograde flow fields of two bileaflet mechanical heart valves. *J Heart Valve Dis* 1996;5:600-606
5. Ellis JT, Travis BR, Yoganathan AP. An in vitro study of the hinge and near-field forward flow dynamics of the St. Jude Medical Regent bileaflet mechanical heart valve. *Ann Biomed Eng* 2000;28:524-532
6. Ellis JT, Yoganathan AP. A comparison of the hinge and near-hinge flow fields of the St. Jude Medical hemodynamic plus and regent bileaflet mechanical heart valves. *J Thorac Cardiovasc Surg* 2000;119:83-93
7. Gross JM, Shu MC, Dai FF, Ellis J, Yoganathan AP. A microstructural flow analysis within a bileaflet mechanical heart valve hinge. *J Heart Valve Dis* 1996;5:581-590
8. Leo HL, He Z, Ellis JT, Yoganathan AP. Microflow fields in the hinge region of the CarboMedics bileaflet mechanical heart valve design. *J Thorac Cardiovasc Surg* 2002;124:561-574
9. Ellis J. An in vitro investigation of the leakage and hinge flow fields through bileaflet mechanical heart valves. PhD Thesis. Georgia Institute of Technology, Atlanta, GA, 1999
10. Travis BR. The effects of bileaflet prosthesis pivot geometry on turbulence and blood damage potential. PhD Thesis. Georgia Institute of Technology, Atlanta, GA, 2001
11. Travis BR, Marzec UM, Leo HL, et al. Bileaflet aortic valve prosthesis pivot geometry influences platelet secretion and anionic phospholipid exposure. *Ann Biomed Eng* 2001;29:657-664
12. Black MM, Drury PJ. Mechanical and other problems of artificial valves. *Curr Top Pathol* 1994;86:127-159
13. Simon H. Influence of the implant location on the hinge and leakage flow fields through bileaflet mechanical heart valves. MSc Thesis. Georgia Institute of Technology, Atlanta, GA, 2004
14. Lu PC, Lai HC, Liu JS. A reevaluation and discussion on the threshold limit for hemolysis in a turbulent shear flow. *J Biomech* 2001;34:1361-1364
15. Hung TC, Hochmuth RM, Joist JH, Sutura SP. Shear-induced aggregation and lysis of platelets. *Trans Am Soc Artif Intern Organs* 1976;22:285-291
16. Ramstack JM, Zuckerman L, Mockros LF. Shear-induced activation of platelets. *J Biomech* 1979;12:113-125
17. Sallam AM, Hwang NH. Human red blood cell hemolysis in a turbulent shear flow: Contribution of Reynolds shear stresses. *Biorheology* 1984;21:783-797
18. Cannegieter SC, Rosendaal FR, Briet E. Thromboembolic and bleeding complications in patients with mechanical heart valve prostheses. *Circulation* 1994;89:635-641
19. Steegers A, Paul R, Reul H, Rau G. Leakage flow at mechanical heart valve prostheses: Improved washout or increased blood damage? *J Heart Valve Dis* 1999;8:312-323
20. Leo H-L. An in vitro investigation of the flow fields through bileaflet and polymeric prosthetic heart valves. PhD Thesis. Georgia Institute of Technology, Atlanta, 2005